

Article

Light-Induced Structures and Microparticle Transportation in a Free-Surface Frustrated Chiral Nematic Film

Sergey A. Shvetsov ^{1,2,*} , Tetiana Orlova ³  and Alexander V. Emelyanenko ¹ ¹ Faculty of Physics, Lomonosov Moscow State University, Moscow 119991, Russia; emel@polly.phys.msu.ru² Lebedev Physical Institute, Russian Academy of Sciences, Moscow 119991, Russia³ Infochemistry Scientific Center, ITMO University, Saint-Petersburg 191002, Russia; torlova@itmo.ru

* Correspondence: shvetsov@polly.phys.msu.ru

Abstract: Local illumination with a light beam leads to thermo-orientational processes in a frustrated chiral nematic film with a free surface. Light-induced hydrodynamic flow and orientational structure create an adaptive platform for the collection, translation and rotation of suspended spherical microparticles. The demonstrated approach has potential applications in soft robotics, micro-object delivery systems, and other micro- and nanotechnologies.

Keywords: chiral liquid crystal; microparticle; optical manipulation; orientational structure; elastic deformation; thermocapillary effect

In the early 2000s, an interest arose in the manipulation of micro- and nanoparticles using liquid crystals (LC), which continues today [1]. This happened due to both the general development of micro- and nanotechnologies in many areas of industry that require precise control of the particle position in the material being designed, their guided assembly and disassembly, and the high responsiveness of the orientational structure of liquid crystals to weak external influences [2]. Microscopic objects can effectively be caught up by the flow of a conventional fluid due to the hydrodynamic effects; while in liquid crystals, the direction of particle motion is additionally regulated by the director field due to the coupling of hydrodynamic and orientational effects [3]. Furthermore, micro- and nanoparticles in LCs readily stick to topological defects, such as disclination lines, or can be trapped by defect structures, such as skyrmions, reducing the total free energy of the system [1]. On the other hand, the liquid crystal orientational structure can be effectively manipulated by external electric and magnetic fields applied to the LC sample, light irradiation, geometric confinement and alignment conditions. Thus, it looks like it is rather easy and reasonable to create a liquid crystal platform—a smart driver of microparticle behavior.

In the field of microscopic object manipulation, a lot of attention has been paid to the electrically induced transport phenomena in nematic liquid crystals, based on electrophoresis and electro-osmosis, electrohydrodynamic convection or backflow powered by director reorientations [4–7]. The presence of either artificially placed or self-generated wall defects allows the microparticles to exhibit a rich set of motions and provide control of their velocity [8,9]. A biotechnological approach involves the use of living liquid crystals, namely swimming bacteria placed in a passive lyotropic chromonic LC and pushing cargo along the trajectory defined by the nematic LC director field [10,11]. However, one could easily imagine a situation where neither the presence of electrical wires nor living objects are suitable for the technology. In this case, the solution may be to remotely control the properties and structure of the liquid crystal by light. The photo-patterned surface alignment [12], which can also be combined with an applied electric field [13], allows one the self-assembly, dynamic behavior and translation of colloids. Another interesting technique lies in designing a self-propelled microparticle by light-induced isomerization of photoresponsive dendrimer molecules adsorbed at the cargo surface [14]. The use of laser traps inducing an optothermal effect is also effective for colloid manipulation [15];



Citation: Shvetsov, S.A.; Orlova, T.; Emelyanenko, A.V. Light-Induced Structures and Microparticle Transportation in a Free-Surface Frustrated Chiral Nematic Film. *Crystals* **2022**, *12*, 549. <https://doi.org/10.3390/cryst12040549>

Academic Editor: Charles Rosenblatt

Received: 22 March 2022

Accepted: 11 April 2022

Published: 14 April 2022

Publisher's Note: MDPI stays neutral with regard to jurisdictional claims in published maps and institutional affiliations.



Copyright: © 2022 by the authors. Licensee MDPI, Basel, Switzerland. This article is an open access article distributed under the terms and conditions of the Creative Commons Attribution (CC BY) license (<https://creativecommons.org/licenses/by/4.0/>).

however, this approach requires precise positioning of the laser beam with respect to the microparticle position or even its well-defined movement [16,17]. In chiral nematic LCs, light-induced topological solitons can involve nearby micro-objects in motion [18] and are themselves involved in motion by them [19].

A rather unexplored research area is related to the use of an open-surface LC film as a transport platform for microparticles. Light-controlled reorganization of a chiral nematic LC film doped with photoresponsive chiral molecules can provide both rotational and translational movement of an embedded micro-object lying on top of an open surface [20,21]. The cargo rotation can also be detected in a free-surface nematic LC film under laser-induced deformation, which causes a thermocapillary flow [22]. This research line remains very intriguing since the absence of a top glass substrate that fixes an LC film should contribute to achieving the highest speed of microparticle transport.

Here, we present an experimental study aimed to demonstrate the microparticle manipulations by light-induced orientational and hydrodynamic processes in an LC environment caused by the action of a laser beam on the frustrated chiral nematic film with a free surface.

To prepare a chiral nematic liquid crystal, the E7 nematic host was doped with 0.2 wt % of the S1011 chiral agent forming a left-handed twist (E7 and S1011 were provided by Synthron Chemicals GmbH & Co. KG, Bitterfeld-Wolfen, Germany). The undeformed cholesteric pitch $p = 15 \mu\text{m}$ was measured by the droplet method [23]. The mixture was deposited onto the indium tin oxide (ITO) coated glass plate to obtain homeotropic anchoring and sufficient wettability, allowing LC to form a relatively thin and stable film [24]. Homeotropic anchoring was also provided spontaneously at the LC–air interface. Thus, in the areas where the LC film thickness L was less than p , the homogeneous untwisted director field was formed, but its orientational structure could be perturbed by the action of a light beam (Figure 1a). In microparticle manipulation experiments, spherical polymer particles with a diameter of $d = 5.5 \mu\text{m}$ (SP-2055, Sekisui Chemical Co., Ltd., Tokio, Japan) dissolved in ethanol were randomly spread onto the glass plate. After ethanol evaporation, an LC layer was deposited on top.

The experimental setup consisted of a continuous-wave laser (SSP-LN-532-FN-300-0.5-LED, CNI, Changchun, China) with the irradiation wavelength $\lambda = 532 \text{ nm}$, a mechanical shutter, and a 75 mm focusing lens (Figure 1b). After focusing the linearly polarized (along X axis) laser beam onto the sample, the beam waist $w_0 = 26 \pm 5 \mu\text{m}$ was measured using the “knife-edge” method [25]. The beam power was measured by a 3664 Hioki power meter (PM). An imaging circuit consisting of an LED with maximum emission intensity at 620 nm, a red color filter (KS10) that absorbs laser irradiation at 532 nm, and a high-speed USB camera with a 16x objective was implemented into the optical setup. The imaging configuration allowed us polarized optical microscopic (POM) observations of liquid crystal textures in crossed or parallel polarizers. The shutter and USB camera were synchronized and controlled by a PC.

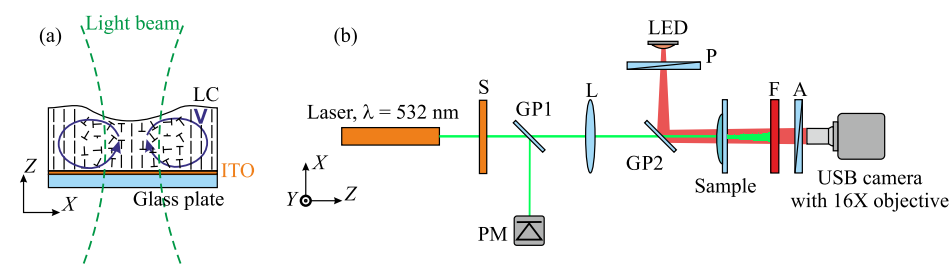


Figure 1. Schematic representation of the LC orientation upon light beam irradiation (a). The dashes and nails show the orientation of the local director; the blue lines show convection flows with velocity V in the XZ plane. Scheme of the experimental setup (b). S—shutter; L—lens; GP1, GP2—glass plates; PM—photodiode optical power meter; P and A—polarizer and analyzer; F—red color filter; LED-1—light emitting diode.

As is known, the light beam passing through an LC sample with an ITO-coated glass substrate is partially absorbed by the ITO layer ($\sim 3\%$ of incident power [24]). A local increase in temperature leads to at least two processes: the pit formation due to the thermo-capillary effect [26] and the temperature-induced deformation of the director field [24,27]. These two processes in a free surface LC film are responsible for the twist director field excitation similar to that induced by direct or indirect light beam action [28–30]. The maximum temperature increase is estimated as $\Delta T = \Delta P / (\sqrt{2\pi\kappa w_0})$ [31], where ΔP is the absorbed power and $\kappa = 10 \text{ mW/cm}^\circ\text{C}$ is the thermal conductivity coefficient of a glass substrate and can reach several tens of degrees in our case. Note that the optical reorientation in the chiral nematic layer can occur because of the dielectric anisotropy at light frequency [32,33]. The laser beam intensity $\sim 1 \text{ kW/cm}^2$ used in our experiment is applicable for direct director reorientation in the LC cell with $L = 150 \mu\text{m}$ [34], but this effect is negligible in nematic films, which are one order of magnitude thinner because the energy of elastic deformation is proportional to $1/L^2$.

We irradiated the chiral nematic free-surface sample in the area where the cholesteric helix is suppressed but in the vicinity of a finger defect, which ensures the metastability of the frustrated state (Figure 2, upper right corner). At the first stage of light illumination with a laser beam power of $P = 43 \text{ mW}$ (peak intensity is $I = 2P/\pi w_0^2 = 4.1 \text{ kW/cm}^2$), the Maltese cross pattern is observed with crossed polarizers similarly to a nematic free-surface film [24]. This corresponds to a radial reorientation of the director with the formation of an umbilical defect [27]. After $\sim 50 \text{ ms}$ of light irradiation, the orientational structure begins to twist, demonstrating a local winding of the cholesteric helix. The cross-polarized optical view of the emerging pattern resembles an individual cholesteric finger loop with 2π director twist, which was observed in a chiral nematic sample with ITO-coated glasses upon local optical realignment and laser-induced heating by a focused light beam [35]. The twisted orientational structure becomes fully developed after a few hundred milliseconds and can only grow slightly thereafter. In the absence of irradiation with a light beam, it relaxes back into the frustrated state in the same couple of hundred milliseconds.

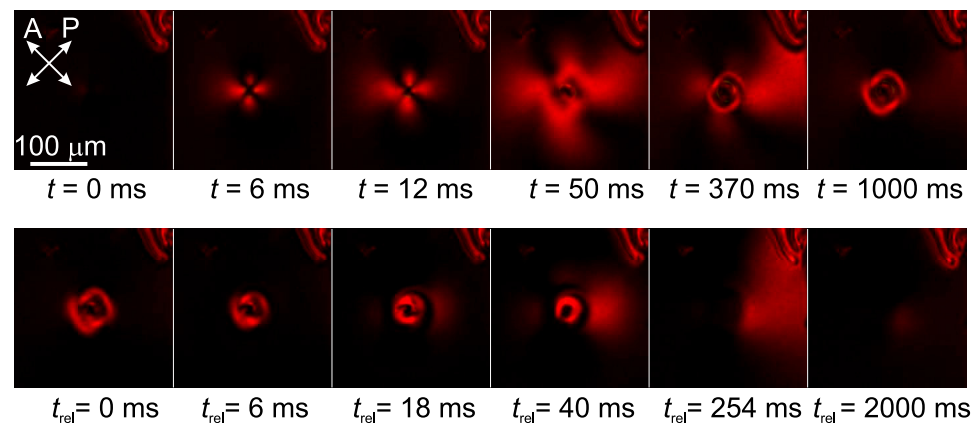


Figure 2. POM images with crossed polarizers of the irradiated area at different time moments t and t_{rel} during and after exposure to the laser beam with a power of $P = 43 \text{ mW}$.

The steady-state deformation of the director field is usually achieved after a couple of minutes of laser beam irradiation and depends significantly on the light intensity I . The sharp Maltese cross pattern is observed when the light power exceeds 15 mW . A bright circular pattern appears at 24 mW and becomes larger as the light power increases further (Figure 3). The deformation area is comparable to the laser beam waist at relatively low intensities but becomes several times larger with the development of the liquid crystal twist configuration.

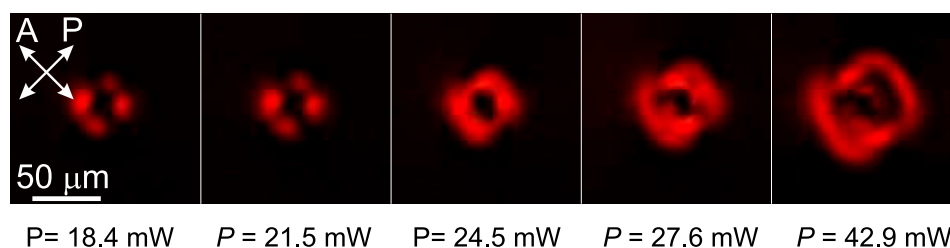


Figure 3. POM images with crossed polarizers of the exposed LC areas after ~ 2 min irradiation with the laser beam of different power P .

In the LC sample doped with polymer microparticles, the light-induced formation of the orientation structure leads to the microparticle trapping and transports from its periphery to the central area (Figure 4a). A number of microparticles can be collected by moving the LC sample along the X-axis. At a sufficiently high power of the laser beam (>42 mW), the microparticle cluster shows off-axis rotation around the center of the twisted structure. The angular velocity depends linearly on the beam power (Figure 4b), demonstrating the conversion of light energy into mechanical work. The Supplementary Video S1 taken with parallel polarizers shows the trapping, transport and beginning of microparticle rotation when a frustrated area of the chiral nematic is illuminated by the laser beam with $P = 51$ mW. The Supplementary Video S2 shows the steady-state off-axis rotation of the microparticle cluster at the laser beam power of $P = 96$ mW.

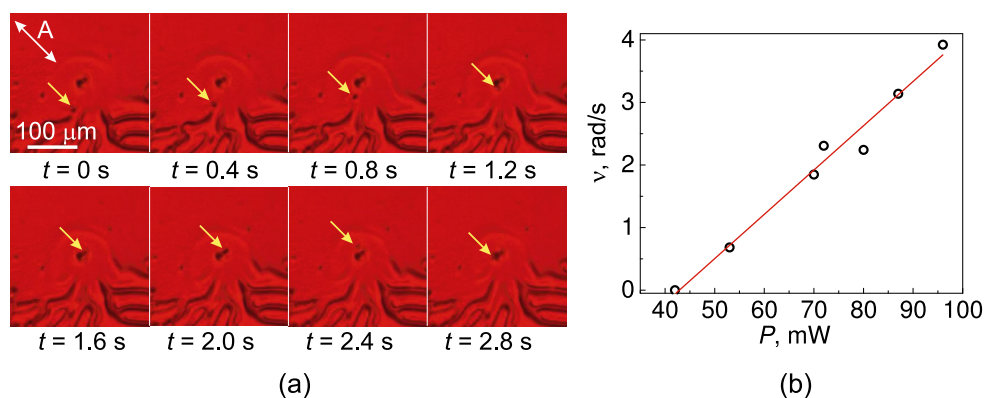


Figure 4. Optical view of the irradiated area with randomly distributed spherical polymer particles in the presence of the analyzer at different exposure times t with the laser beam of $P = 96$ mW (a). The position of the moving particle is marked with yellow arrows. The textures in the lower part of each image correspond to the area of cholesteric finger defects. The microparticle is trapped and moves to the center of the orientation twisted structure along an arc trajectory. Linear dependence of the angular velocity on the laser beam power (b).

Our experiments seem to show that effective particle transport can only be achieved at a certain ratio of the size of the twisted structure and the particle diameter. For larger microparticles with a diameter of $d = 8.5$ μm embedded in the chiral nematic LC with the cholesteric pitch $p = 15$ μm , the transport effect is suppressed. For the same microparticles in the chiral nematic LC with the cholesteric pitch $p = 25$ μm , the effect is weak for any thickness of the LC layer from 0 to 25 μm , and even more, it looks like a pushing of microparticles from the irradiated area prevails.

We propose the following explanation of the effects observed. As it is known, hydrodynamic flows and the LC director field deformation are coupled to each other [3]. The pit in the LC film, induced by thermocapillary forces due to the light absorption by the ITO layer and the corresponding temperature gradient, is further supported by convection flows with a velocity field in the form of closed lines (Figure 1a). However, while the hydrodynamic

flow can be easily established near the free surface of the LC film, the flow near the solid bottom substrate is limited by the positional anchoring of LC molecules. The velocity flux out of the center of the light-induced pit should be compensated by the reversed one, which is supposed to be responsible for the microparticle collection and motion. At the same time, local defrustration of the LC film leads to the twisted orientational structure that directs the microparticle movement along a curved trajectory in the XY plane. The rotation direction of a microparticle cluster is determined by the twist of the orientational structure. Of course, specific mechanisms of microparticle transport due to hydrodynamic flows coupled with twisted configurations of the director field require further study.

The modest values of the angular velocity (Figure 4b) are understandable when taking into account that a whole cluster of microparticles rotates. These values should become higher in the case of single microparticle rotation, similarly to [22]. On the other hand, we demonstrate the principal possibility of manipulating a microparticle cluster due to the combined action of hydrodynamic effects and twisted orientational structures, while previously, the local chiral patterns were used only to control the behavior of a single cargo [18,19]. Further development of the presented approach will contribute to the implementation of high-speed transportation of a single micro-object using a light-controlled soft platform for various technological applications that require smart delivery systems.

Supplementary Materials: The following supporting information can be downloaded at: <https://www.mdpi.com/article/10.3390/cryst12040549/s1>. SM1 video demonstrates the possibility of the microparticle transport and rotation when a frustrated area of the chiral nematic is illuminated by the laser beam with $P = 51$ mW, SM2 video shows the steady-state rotation of the microparticle cluster at the laser beam power of $P = 96$ mW.

Author Contributions: Conceptualization, S.A.S. and T.O.; investigation, S.A.S.; resources, A.V.E.; writing—original draft preparation, S.A.S. and T.O.; writing—review and editing, S.A.S. and T.O.; supervision, A.V.E.; funding acquisition, S.A.S. All authors have read and agreed to the published version of the manuscript.

Funding: This research was funded by the Russian Science Foundation, Grant No. 20-72-00178.

Data Availability Statement: The data could be obtained from the corresponding author.

Acknowledgments: T.O. acknowledges the support from the Government of the Russian Federation through the ITMO Professorship and Fellowship program. S.A.S. and A.V.E. acknowledge partial support from M.V.Lomonosov Moscow State University Program of Development.

Conflicts of Interest: The authors declare no conflict of interest.

References

1. Lagerwall, J.P.F.; Scalia, G. *Liquid Crystals with Nano and Microparticles*; Series in Soft Condensed Matter; World Scientific: Singapore, 2016; Volume 7. [CrossRef]
2. Oswald, P.; Pieranski, P. *Nematic and Cholesteric Liquid Crystals: Concepts and Physical Properties Illustrated by Experiments*; CRC Press: Boca Raton, FL, USA, 2005.
3. Blinov, L.M. *Structure and Properties of Liquid Crystals*; Springer: Dordrecht, The Netherlands, 2011. [CrossRef]
4. Lavrentovich, O.D. Transport of particles in liquid crystals. *Soft Matter* **2014**, *10*, 1264–1283. [CrossRef]
5. Sasaki, Y.; Takikawa, Y.; Jampani, V.S.R.; Hoshikawa, H.; Seto, T.; Bahr, C.; Herminghaus, S.; Hidaka, Y.; Orihara, H. Colloidal caterpillars for cargo transportation. *Soft Matter* **2014**, *10*, 8813–8820. [CrossRef]
6. Nishioka, Y.; Kobayashi, F.; Sakurai, N.; Sasaki, Y.; Orihara, H. Microscopic characterisation of self-assembled colloidal particles in electrohydrodynamic convection of a low-birefringence nematic liquid crystal. *Liq. Cryst.* **2016**, *43*, 427–435. [CrossRef]
7. Li, B.X.; Xiao, R.L.; Shiyankovskii, S.V.; Lavrentovich, O.D. Soliton-induced liquid crystal enabled electrophoresis. *Phys. Rev. Res.* **2020**, *2*, 013178. [CrossRef]
8. Bhadwal, A.S.; Mottram, N.J.; Saxena, A.; Sage, I.C.; Brown, C.V. Electrically controlled topological micro cargo transportation. *Soft Matter* **2020**, *16*, 2961–2970. [CrossRef] [PubMed]
9. Luo, Y.; Beller, D.A.; Boniello, G.; Serra, F.; Stebe, K.J. Tunable colloid trajectories in nematic liquid crystals near wavy walls. *Nat. Commun.* **2018**, *9*, 3841. [CrossRef]
10. Lavrentovich, O.D. Active colloids in liquid crystals. *Curr. Opin. Colloid Interface Sci.* **2016**, *21*, 97–109. doi:10.1016/j.cocis.2015.11.008. [CrossRef]

11. Trivedi, R.R.; Maeda, R.; Abbott, N.L.; Spagnolie, S.E.; Weibel, D.B. Bacterial transport of colloids in liquid crystalline environments. *Soft Matter* **2015**, *11*, 8404–8408. [[CrossRef](#)]
12. Peng, C.; Turiv, T.; Guo, Y.; Shiyanovskii, S.V.; Wei, Q.H.; Lavrentovich, O.D. Control of colloidal placement by modulated molecular orientation in nematic cells. *Sci. Adv.* **2016**, *2*, e1600932. [[CrossRef](#)]
13. Straube, A.V.; Pagès, J.M.; Ortiz-Ambriz, A.; Tierno, P.; Ignés-Mullol, J.; Sagués, F. Assembly and transport of nematic colloidal swarms above photo-patterned defects and surfaces. *New J. Phys.* **2018**, *20*, 075006. [[CrossRef](#)]
14. Eremin, A.; Hirankittiwong, P.; Chattham, N.; Nádas, H.; Stannarius, R.; Limtrakul, J.; Haba, O.; Yonetake, K.; Takezoe, H. Optically driven translational and rotational motions of microrod particles in a nematic liquid crystal. *Proc. Natl. Acad. Sci. USA* **2015**, *112*, 1716–1720. [[CrossRef](#)]
15. Fuh, A.Y.G.; Li, M.H.; Chang, T.W.; Lee, Y.I.; Wu, S.T. Optical manipulation of nematic colloids at the interfaces in azo-dye-doped liquid crystals. *Appl. Opt.* **2018**, *57*, 3180–3185. [[CrossRef](#)] [[PubMed](#)]
16. Škarabot, M.; Lokar, Ž.; Muševič, I. Transport of particles by a thermally induced gradient of the order parameter in nematic liquid crystals. *Phys. Rev. E* **2013**, *87*, 062501. [[CrossRef](#)] [[PubMed](#)]
17. Škarabot, M.; Osterman, N.; Muševič, I. Optothermally driven colloidal transport in a confined nematic liquid crystal. *Soft Matter* **2017**, *13*, 2448–2452. [[CrossRef](#)]
18. Orlova, T.; Lancia, F.; Loussert, C.; Iamsaard, S.; Katsonis, N.; Brasselet, E. Revolving supramolecular chiral structures powered by light in nanomotor-doped liquid crystals. *Nat. Nanotechnol.* **2018**, *13*, 304–308. [[CrossRef](#)]
19. Porenta, T.; Čopar, S.; Ackerman, P.J.; Pandey, M.B.; Varney, M.C.M.; Smalyukh, I.I.; Žumer, S. Topological Switching and Orbiting Dynamics of Colloidal Spheres Dressed with Chiral Nematic Solitons. *Sci. Rep.* **2015**, *4*, 7337. [[CrossRef](#)] [[PubMed](#)]
20. Eelkema, R.; Pollard, M.M.; Katsonis, N.; Vicario, J.; Broer, D.J.; Feringa, B.L. Rotational Reorganization of Doped Cholesteric Liquid Crystalline Films. *J. Am. Chem. Soc.* **2006**, *128*, 14397–14407. [[CrossRef](#)]
21. Kausar, A.; Nagano, H.; Ogata, T.; Nonaka, T.; Kurihara, S. Photocontrolled Translational Motion of a Microscale Solid Object on Azobenzene-Doped Liquid-Crystalline Films. *Angew. Chem. Int. Ed.* **2009**, *48*, 2144–2147. [[CrossRef](#)] [[PubMed](#)]
22. Choi, H.; Takezoe, H. Circular flow formation triggered by Marangoni convection in nematic liquid crystal films with a free surface. *Soft Matter* **2016**, *12*, 481–485. [[CrossRef](#)] [[PubMed](#)]
23. Solladié, G.; Zimmermann, R.G. Liquid Crystals: A Tool for Studies on Chirality. *Angew. Chem. Int. Ed. Engl.* **1984**, *23*, 348–362. [[CrossRef](#)]
24. Shvetsov, S.A.; Zolot'ko, A.S.; Voronin, G.A.; Emelyanenko, A.V.; Avdeev, M.M.; Bugakov, M.A.; Statsenko, P.A.; Trashkeev, S.I. Light-induced umbilical defects due to temperature gradients in nematic liquid crystal with a free surface. *Opt. Mater. Express* **2021**, *11*, 1705. [[CrossRef](#)]
25. Khosrofiyan, J.M.; Garetz, B.A. Measurement of a Gaussian laser beam diameter through the direct inversion of knife-edge data. *Appl. Opt.* **1983**, *22*, 3406. [[CrossRef](#)] [[PubMed](#)]
26. Zykov, A.Y.; Ivanova, N.A. Laser-induced thermocapillary convection in thin liquid layers: effect of thermal conductivity of substrates. *Appl. Phys. B* **2017**, *123*, 235. [[CrossRef](#)]
27. Shvetsov, S.; Zolot'ko, A.; Voronin, G.; Emelyanenko, A.; Statsenko, P.; Trashkeev, S. Coexistence of light-induced thermocapillary and orientational effects in thin nematic films with a free surface. *J. Phys. Conf. Ser.* **2021**, *2067*, 012016. [[CrossRef](#)]
28. Smalyukh, I.I.; Lansac, Y.; Clark, N.A.; Trivedi, R.P. Three-dimensional structure and multistable optical switching of triple-twisted particle-like excitations in anisotropic fluids. *Nat. Mater.* **2010**, *9*, 139–145. [[CrossRef](#)]
29. Loussert, C.; Brasselet, E. Multiple chiral topological states in liquid crystals from unstructured light beams. *Appl. Phys. Lett.* **2014**, *104*, 051911. [[CrossRef](#)]
30. Shvetsov, S.; Orlova, T.; Emelyanenko, A.V.; Zolot'ko, A. Thermo-Optical Generation of Particle-Like Structures in Frustrated Chiral Nematic Film. *Crystals* **2019**, *9*, 574. [[CrossRef](#)]
31. Abraham, E.; Ogilvy, I.J.M. Heat flow in interference filters. *Appl. Phys. B Photophysics Laser Chem.* **1987**, *42*, 31–34. [[CrossRef](#)]
32. Abbate, G.; Maddalena, P.; Marrucci, L.; Saetta, L.; Ferraiuolo, A.; Ferraiuolo, S.; Santamato, E. First-Order Optical Fréedericksz Transition in Nematics Doped with Chiral Agents. *Mol. Cryst. Liq. Cryst. Sci. Technol. Sect. A Mol. Cryst. Liq. Cryst.* **1992**, *223*, 11–18. [[CrossRef](#)]
33. Abbate, G.; Ferraiuolo, A.; Maddalena, P.; Marrucci, L.; Santamato, E. Optical reorientation in cholesteric nematic mixtures. *Liq. Cryst.* **1993**, *14*, 1431–1438. [[CrossRef](#)]
34. Kitaeva, V.F.; Zolot'ko, A.S.; Sobolev, N.N. Self-focusing of laser radiation in the case of a Fredericks transition. *Phys. Usp.* **1982**, *25*, 758–760. [[CrossRef](#)]
35. Ackerman, P.J.; Trivedi, R.P.; Senyuk, B.; van de Lagemaat, J.; Smalyukh, I.I. Two-dimensional skyrmions and other solitonic structures in confinement-frustrated chiral nematics. *Phys. Rev. E* **2014**, *90*, 012505. [[CrossRef](#)] [[PubMed](#)]